Japanese Journal of
Applied Physics

Water Trapping at the Graphene/Al_2O_3 Interface

Japanese Journal of Applied Physics **52** (2013) 06GD09 **REGULAR PAPER**
http://dx.doi.org/**10.7567/JJAP.52.06GD09**

Water Trapping at the Graphene/Al_2O_3 Interface

Sung Beom Cho, Sangho Lee, and Yong-Chae Chung*

Department of Materials Science and Engineering, Hanyang University, Seoul 133-791, Korea
E-mail: yongchae@hanyang.ac.kr

Received December 5, 2012; accepted February 8, 2013; published online June 20, 2013

We investigated the effects of trapped water at the graphene/Al_2O_3 interface using density functional theory. We found that molecularly trapped water does not induce serious interbanding at the Dirac point. However, dissociatively trapped water induces serious interbanding at the Dirac point because of the band alignment induced by the local field of the hydroxyl groups. These findings indicate that trapped water at the graphene/Al_2O_3 interface can have a significant effect on the electronic structure of graphene. © 2013 The Japan Society of Applied Physics

1. Introduction

Graphene is a two-dimensional sheet of sp^2-hybridized carbon atoms arranged in a honeycomb structure, that enables the formation of the long-range π conjugation network in the sheet.[1,2] Obeying Dirac's relativistic equation, the π and π^* bands of graphene display linear dispersion with extremely high electron mobility, showing zero effective mass.[3] The high electron mobility and two-dimensionality of graphene makes it an ideal material for use in electronic devices.[4] In recent years, several types of graphene-based devices have been proposed, such as field-effect transistors,[5,6] floating-gate flash memory,[7] and charge-trap memory.[8] For these types of graphene-based electronics, Al_2O_3 is considered an ideal dielectric substrate or gate material because of its high dielectric constant, large injection barrier [i.e., large band offset (>2 eV) with respect to graphene,[9] and chemical stability.[10] According to recent first-principle calculation performed by Ilyasov et al.,[11] the graphene is weakly physisorbed on Al_2O_3 substrate. Due to the weak interaction and large band offset, the band of graphene near the Dirac point is relatively well preserved. Furthermore, it has been reported by Huang et al. that a remarkable band gap of 180 meV can be induced in a graphene layer adsorbed on an Al-terminated Al_2O_3 surface. This is a huge advantage for enhancing the on/off ratio of a device.[12] Because Al_2O_3 can be grown by atomic layer deposition (ALD), its thickness can be controlled, compositional uniformity can be obtained, and a low temperature process can be used.

Water is often employed as the oxidizing agent during ALD.[13] Because Al_2O_3 can be exposed in humid conditions during the fabrication process, an adsorbed water molecule can remain on the surface. Furthermore, water adlayers can be trapped beneath the graphene when the graphene is exposed to ambient atmosphere.[14] Therefore, H_2O can be trapped at the graphene/Al_2O_3 interface during the deposition or transfer process of the fabrication. Such water trapping can also occur at pentacene/SiO_2[15] and graphene/SiO_2[16,17] interfaces, and can induce hole trapping or inter-banding. In particular, trapped water at the graphene/SiO_2 interface has an important influence on the hysteresis loop of the graphene based field-effect transistor.[18] The effect of trapped water at graphene/SiO_2 has attracted much of discussion.[19,20] However, relatively little is known about trapped water and its effect at the graphene/Al_2O_3 interface.

We therefore investigated whether trapped water molecules are present at the graphene/Al_2O_3 interface using density functional theory (DFT)-based ab-initio calculations. In particular, we determined the adhesion character and electronic structure of graphene on Al_2O_3 with molecularly adsorbed water and dissociatively adsorbed water. In addition, we investigated the effect of trapped water by saturation coverage.

2. Calculation Details

First-principles calculations were based on the Kohn–Sham equation as implemented in the Vienna ab-initio simulation package code (VASP).[21] The projector augmented wave (PAW) method[22] was used to describe the ionic potentials, and the exchange–correlation function between the electrons was adopted for the Perdew–Burke–Ernzerhof (PBE) potential.[23] The effect of the van der Waals interactions was modeled by employing the empirical correction scheme of Grimme (DFT-D2),[24] which has been proven to be successful at describing the geometries of graphene-related structures.[25,26] The basis set of the plane waves was expanded up to a cutoff energy of 400 eV and Gaussian smearing was used with a sigma value of 0.2 eV.

The Al_2O_3 surface was modeled by a 12-layer-thick slab [four complete Al(O_3)Al layers] containing two unit cells in the lateral directions. The five bottom layers of the Al_2O_3 layers were kept fixed at their optimized bulk positions. The surface layers, adsorbates, and graphene layers were fully relaxed until the maximum Hellmann–Feynman forces were in the range of 0.03 eV/Å. The vacuum thickness was set to at least 18 Å, and a dipole correction was used for all calculations. A first Brillouin-zone integration scheme was used on a grid of $(7 \times 7 \times 1)$ Γ-centered Monkhorst–Pack points.[27] From the calculated electronic structure, the planar-averaged charge density was evaluated by

$$\rho(z) = \iint_A \rho(x, y, z)\, dx\, dy. \quad (1)$$

Furthermore, the interface was calculated according to

$$E_{\text{interface}} = E_{\text{grpn/H}_2\text{O/Al}_2\text{O}_3} - E_{\text{grpn}} - E_{\text{substrate}}. \quad (2)$$

3. Results and Discussion

Under ultrahigh vacuum conditions, it has been reported that the most stable surface structure of α-Al_2O_3 is the top layer of Al_s cations and the hexagonal array of the second-layer O_s anions.[28] Because Al_s is undercoordinated on the surface, it

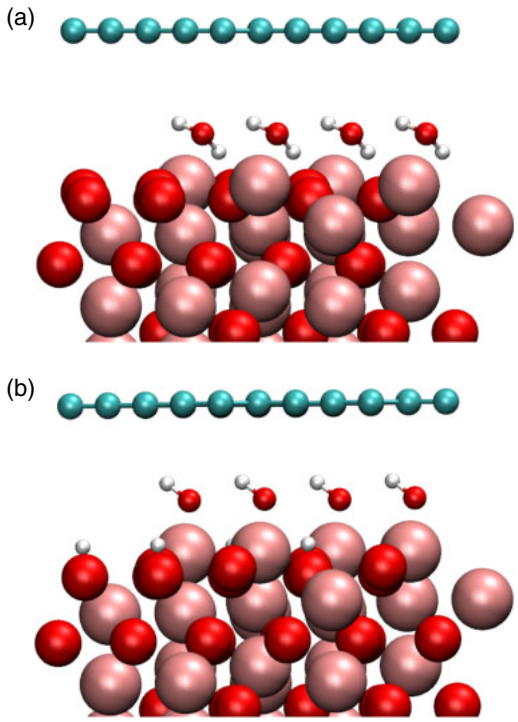

Fig. 1. (Color online) Side view of graphene on Al_2O_3 with (a) molecularly adsorbed water and (b) dissociatively adsorbed water. The red, pink, white, and cyan spheres represent O, Al, H, and C atoms, respectively.

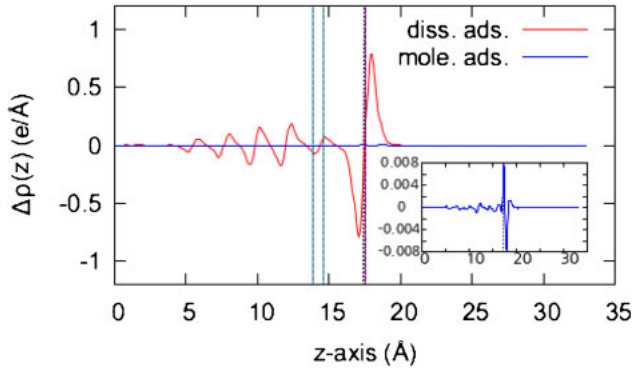

Fig. 2. (Color online) Planar averaged charge density difference of graphene on Al_2O_3 with (a) molecularly adsorbed water and (b) dissociatively adsorbed water. The purple dotted line indicates the position of the graphene layer. The right green dashed line represents the top-most atom of OH of the dissociated water and the left green dashed line represents the top-most atom of H_2O of the molecular adsorbed water.

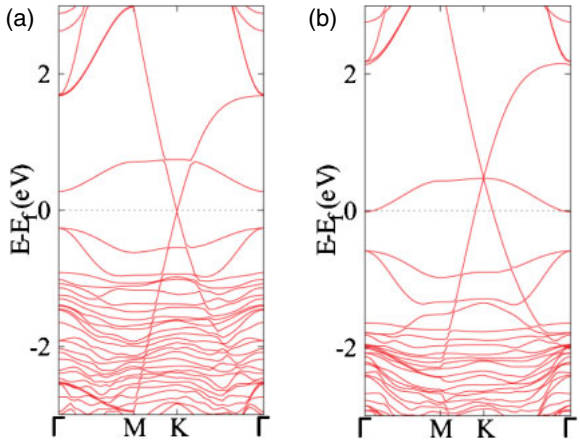

Fig. 3. (Color online) Band structure of graphene on Al_2O_3 with (a) molecularly adsorbed water and (b) dissociatively adsorbed water.

functions as a Lewis acidic adsorption site, i.e., an electron acceptor. These Al_s sites are the preferred adsorption sites for single molecules of water (one per site), with two experimentally observed adsorption modes.[29–31] One is the molecular adsorption to the Al_s sites through binding of the O atom of the water with a binding energy of 1.19 eV. The other mode is dissociative adsorption, splitting of the water into an OH^- fragment atop Al_s and a H^+ fragment atop O_s. The binding energy of the dissociative water is 1.69 eV, which indicates that dissociative adsorption is the more stable adsorption mode. At the graphene/Al_2O_3 interface, both modes of adsorbed water can be trapped.

A side view of graphene on Al_2O_3 with molecularly and dissociatively adsorbed water is shown in Fig. 1. The molecularly adsorbed water molecule is aligned relatively parallel to the surface and one of its hydrogens is directed towards the O_s of Al_2O_3. The distance between the graphene and the top-most atom of the molecularly adsorbed H_2O is 3 Å. In contrast, the hydroxyl group of the dissociated water is aligned relatively perpendicular to the surface and the distance to graphene (2.5 Å) is nearer than that of the molecularly adsorbed H_2O. This is because the hydroxyl group of the dissociated water generates a strong local field that attracts graphene. This was obvious when analyzing the planar-averaged charge density of the interface. The planar-averaged charge density difference between the interface and the sum of the graphene and the substrate (water-adsorbed Al_2O_3) is shown in Fig. 2. The dissociative adsorbed water generates large charge fluctuations in the graphene and the Al_2O_3 substrate. However, the region of fluctuation does not include other atomic regions, which means that there is no charge transfer. This suggests that the mechanism of adhesion is mainly the van der Waals interactions. Similar charge fluctuations occurred for graphene on Al_2O_3 with molecularly adsorbed water, but the scale of the fluctuations was less than two orders of magnitude that of the dissociative adsorbed water. Therefore, the adhesion of graphene and dissociated water is strongly attractive (−0.47 meV/C), while the adhesion of molecularly adsorbed water is slightly repulsive (0.12 meV/C).

The band structure of graphene on Al_2O_3 with trapped water is shown in Fig. 3. The highest occupied molecular orbital of H_2O and OH is more than 1.3 eV below the Fermi energy and its lowest unoccupied molecular orbital is more than 2 eV above the Fermi energy. However, the strong local field generated by the trapped water can have a significant effect on the band structure of graphene. In the case of graphene on Al_2O_3 with molecular adsorbed water, the Dirac point is still at the Fermi level. The band of O_s lies close to the Fermi level but it does not interband at the Dirac point. In contrast, the local field of the dissociated water induced p-type doping of the graphene band and interband with the band of O_s. This interbanding could result in serious degradation of the electronic properties of graphene.

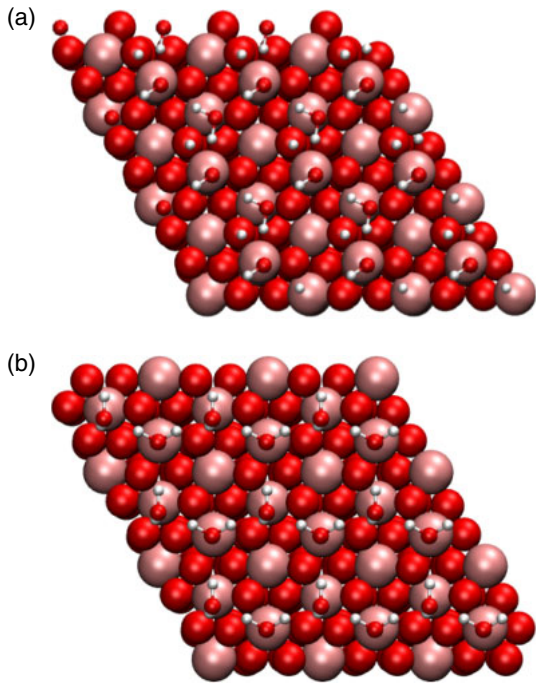

Fig. 4. (Color online) Top view of Al_2O_3 with saturated coverage of (a) 1 : 1 of molecularly and dissociatively adsorbed water and (b) molecularly adsorbed water.

In addition, we calculated the band structure of graphene on Al_2O_3 with saturated coverage of the adsorbed water. Because a water layer can be deposited onto the Al_2O_3 layer,[32] it is important to investigate whether the interbanding trends we observed still occurred. Figure 4 shows the configuration of Al_2O_3 with a saturated coverage of 1 : 1 of molecularly and dissociatively adsorbed water and molecularly adsorbed water, respectively.

In the mixed configuration of molecular and dissociative adsorbtion, a hexagonal network was formed between the hydroxyl group and the molecularly adsorbed H_2O. The direction of the hydroxyl group was still relatively perpendicular to the surface, occupying the Al_s site, while detached hydrogen occupied the O_s site. In contrast, molecularly adsorbed water in the mixed configuration was parallel to the surface, occupying the intermediate position of the hydroxyl group. This indicates that the local field generated by the mixed adsorption configuration was similar to that of the dissociative-only adsorption configuration. Therefore, the band structure of graphene on Al_2O_3 with the mixed adsorption configuration is similar to that of graphene on Al_2O_3 with dissociatively adsorbed water and it also shows interbanding, as illustrated in Fig. 5(a).

In the case of the saturated coverage of the molecularly adsorbed water, the water also formed a hexagonal network, but with a slightly different configuration to that observed previously. The half water was adsorbed through O to Al_s, parallel to the surface. The other half was adsorbed though H to O_s, perpendicular to the surface. Those configurations generated a much weaker surface field with a direction opposite that of the hydroxyl group. Therefore, graphene on Al_2O_3 with saturated coverage of molecularly adsorbed water is slightly n-type doped and does not have interbanding, as shown in Fig. 5(b).

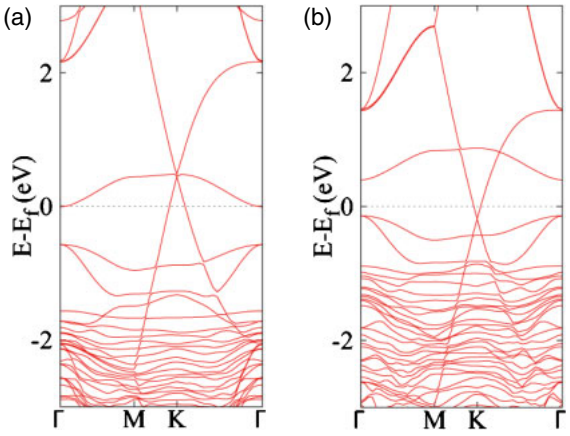

Fig. 5. (Color online) Band structure of graphene on Al_2O_3 with saturated coverage of (a) 1 : 1 of molecularly and dissociatively adsorbed water and (b) molecularly adsorbed water.

4. Conclusions

We investigated the configuration of trapped water at the graphene/Al_2O_3 interface and its effect on the band structure. On the one hand, molecularly adsorbed water on Al_2O_3 did not result in interbanding and the Dirac point was preserved. On the other hand, dissociatively adsorbed water at the interface resulted in interbanding because of the band alignment of the local field generated. Similar trends were observed for the saturated coverage of the water adsorption. In the mixed configuration of the molecular and dissociative adsorption, interbanding was still observed. For the case of saturated coverage of molecularly adsorbed water, no interbanding occurred. Our results provide insight into the effect of trapped water at the graphene/Al_2O_3 interface.

Acknowledgments

This work was supported by a grant from the National Research Foundation (NRF) of Korea funded by the Korean Ministry of Education, Science and Technology (No. 2012-0016945), a Global Ph. D. Fellowship from the National Research Foundation (NRF), and the Basic Science Research Program of the NRF funded by the MEST (No. 2012-0026175).

1) M. J. Allen, V. C. Tung, and R. B. Kanar: Chem. Rev. **110** (2010) 132.
2) A. H. Castro Neto, F. Guinea, N. M. R. Peres, K. S. Novoselov, and A. K. Geim: Rev. Mod. Phys. **81** (2009) 109.
3) K. S. Novoselov, A. K. Geim, S. V. Morozov, D. Jiang, M. I. Katsnelson, I. V. Grigorieva, S. V. Dubonos, and A. A. Firsov: Nature **438** (2005) 197.
4) J. Basu, J. K. Basu, and T. K. Bhattacharyya: Int. J. Smart Nano Mater. **1** (2010) 201.
5) S. Kim, J. Nah, I. Jo, D. Shahrjerdi, L. Colombo, Z. Yao, E. Tutuc, and S. K. Banerjee: Appl. Phys. Lett. **94** (2009) 062107.
6) M.-H. Jung, H. Handa, R. Takahashi, H. Fukidome, T. Suemitsu, T. Otsuji, and M. Suemitsu: Jpn. J. Appl. Phys. **50** (2011) 070111.
7) A. J. Hong, E. B. Song, H. S. Yu, M. J. Allen, J. Kim, J. D. Fowler, J. K. Wassei, Y. Park, Y. Wang, J. Zou, R. B. Kaner, B. H. Weiller, and K. L. Wang: ACS Nano **5** (2011) 7812.
8) S. Lee, E. B. Song, S. Kim, D. H. Seo, S. Seo, T. W. Kang, and K. L. Wang: Appl. Phys. Lett. **100** (2012) 023109.
9) S. Dueñas, H. Castán, H. García, A. de Castro, L. Bailón, K. Kukli, A. Aidla, J. Aarik, H. Mändar, T. Uustare, J. Lu, and A. Hårsta: J. Appl. Phys. **99** (2006) 054902.
10) S. Jakschik, U. Schroeder, T. Hecht, M. Gutsche, H. Seidl, and J. W.

Bartha: Thin Solid Films **425** (2003) 216.
11) V. V. Ilyasov and I. V. Ershov: Phys. Solid State **54** (2012) 2335.
12) B. Huang, Q. Xu, and S.-H. Wei: Phys. Rev. B **84** (2011) 155406.
13) S. M. George: Chem. Rev. **110** (2010) 111.
14) K. Xu, P. Cao, and J. R. Heath: Science **329** (2010) 1188.
15) C. Goldmann, D. J. Gundlach, and B. Batlogg: Appl. Phys. Lett. **88** (2006) 063501.
16) T. O. Wehling, A. I. Lichtenstein, and M. I. Katsnelson: Appl. Phys. Lett. **93** (2008) 202110.
17) J. Moser, A. Verdaguer, D. Jiménez, A. Barreio, and A. Batchtold: Appl. Phys. Lett. **92** (2008) 123507.
18) Z.-M. Liao, B.-H. Han, Y.-B. Zhou, and D.-P. Yu: J. Chem. Phys. **133** (2010) 044703.
19) Y. M. Shi, W. J. Fang, K. K. Zhang, W. J. Zhang, and L. J. Li: Small **5** (2009) 2005.
20) Y. Dan, Y. Lu, N. J. Kybert, Z. Luo, and A. T. C. Johnson: Nano Lett. **9** (2009) 1472.
21) G. Kresse and J. Furthmüller: Comput. Mater. Sci. **6** (1996) 15.
22) G. Kresse and D. Joubert: Phys. Rev. B **59** (1999) 1758.
23) J. P. Perdew, K. Burke, and M. Ernzerhof: Phys. Rev. Lett. **77** (1996) 3865.
24) S. Grimme: J. Comput. Chem. **27** (2006) 1787.
25) G. Mercurio, E. R. McNellis, I. Martin, S. Hagen, F. Leyssner, S. Soubatch, J. Meyer, M. Wolf, P. Tegeder, F. S. Tautz, and K. Reuter: Phys. Rev. Lett. **104** (2010) 036102.
26) D. Stradi, S. Barja, C. Diaz, M. Garnica, B. Borca, J. J. Hinarejos, D. Sanchez-Portal, M. Alcami, A. Arnau, A. L. Vazquez de Parga, R. Miranda, and F. Martin: Phys. Rev. Lett. **106** (2011) 186102.
27) H. J. Monkhorst and J. D. Pack: Phys. Rev. B **13** (1976) 5188.
28) J. Ahn and J. W. Rabalais: Surf. Sci. **388** (1997) 121.
29) P. Liu, T. Kendelewicz, G. E. Brown, E. J. Nelson, and S. A. Chambers: Surf. Sci. **417** (1998) 53.
30) D. B. Almy, D. C. Foyt, and J. M. White: J. Electron Spectrosc. Relat. Phenom. **11** (1977) 129.
31) V. A. Ranea, W. F. Schneider, and I. Carmichael: Surf. Sci. **602** (2008) 268.
32) G. Tzvetkov, Y. Zubavichus, G. Koller, Th. Schmidt, C. Heske, E. Umbach, M. Grunze, M. G. Ramsey, and F. P. Netzer: Surf. Sci. **543** (2003) 131.